Available online at **www.joac.info**

ISSN: 2278-1862

Journal of Applicable Chemistry

2023, 12 (2): 122-129

(International Peer Reviewed Journal)

A study on the effect of 2, 5-dihydroxy benzaldehyde on Electrodeposition of Zinc-Nickel alloy

Nagabhushana[1]*, G. P. Mamatha[2], S. Basavanna[3]

1. Department of Chemistry, Kuvempu University, Shankaraghatta-577451 Karnataka, **INDIA**
2. Department of Chemistry, Davanagere University, Shivagangotri, Davanagere-577002, Karnataka, **INDIA**
3. Department of Chemistry, Prerana PU College, Tumkur-572102, Karnataka, **INDIA**

Email: nagabhushanaspatil1980@gmail.com

Accepted on 11th March, 2023

ABSTRACT

An organic additive, 2, 5 dihydroxy benzaldehyde (DHB), was used for the electrodeposition of Zn-Ni alloy from a sulphate bath. The cyclic voltammetry was used to study the electrodeposition process while electrochemical impedance spectroscopy and potentiodynamic polarization techniques were used to investigate corrosion. The Zn-Ni-bright deposit obtained is more uniform, fine-grained, and corrosion-resistant than the Zn-Ni-dull deposit. The morphology and phase of the deposits were studied using scanning electron microscopy and X-ray diffraction.

Graphical Abstract:

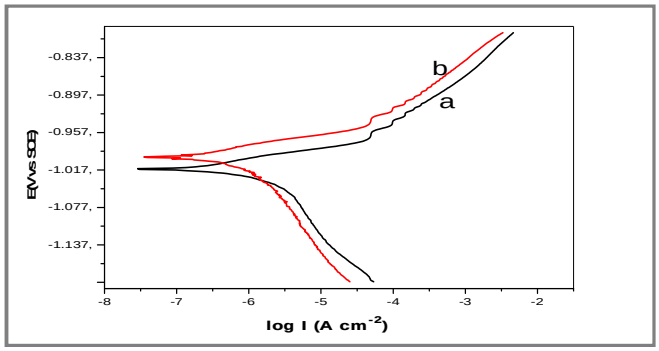

Typical Tafel plots of Zn- Ni alloy electrodeposits in 3.5 % NaCl solution obtained (A) in absence and (B) in presence of DHB in the bath solution.

Keywords: Zn-Ni alloy, Electrodeposition, Cyclic voltammetry, Phase structure.

INTRODUCTION

Electrodeposition of Zinc alloy has gained more prominence because it offers an improved corrosion barrier compared to electro-galvanized coatings [**1-3**]. Zn-Ni layers protect steel effectively, the highest protecting capacity is achieved at a nickel concentration of 14%, depending on the content of the bath and working conditions. “Brenner [**3**] categorizes the electrode position of Zn-Ni alloys as an

anomalous co-deposition", in which zinc is less noble, and is deposited preferentially. Even though this phenomenon was already recognized, the mechanism of Zn-Ni co-deposition [**4, 5**] remains unclear. The anomalous co-deposition of Zn-Ni alloys has been the subject of several theories. The former relates the anomalous co-deposition to an increase in local pH, which may lead to the precipitation of zinc hydroxide and prevent nickel deposition [**6**]. Zn-Ni alloy plating baths can be either acidic or alkaline [**7**], and these two varieties are the most common. An acid bath is composed of salts of zinc and nickel electrolytes, buffers, and also sometimes brighteners. The alkaline type electrolyte contains NaOH, additives, and metallic ions. Zn-Ni alloys exist in a variety of phases, and it is well-accepted that the structure and morphology of a deposit can impact its corrosion resistance [**8**].

The inclusion of additives in electroplating baths is crucial because they influence the development and morphology of the deposits formed. Additives are frequently involved to the electrolytic solution in parts per million; their inclusion improves the formation of uniform and lustrous surfaces [**9-11**]. Additives attaching to the electrode superficial might change the activation energy [**12**], the velocity of charge transfer during the electrolytic process as well as the electro-crystallization mechanism [**13**]. Moreover, the additives close some of the active sites on the cathode surface, which lowers the rate of nucleation [**14, 15**].

Thus in the current case, an organic additive 2, 5 dihydroxy benzaldehyde (DHB) has been utilized for Zn-Ni alloy electrodeposition on low-carbon steel from acid sulfates.

MATERIALS AND METHODS

The Zn-Ni alloy electroplating bath was made using distilled water and chemicals suitable for use in laboratories. The bath composition and operation parameters (Table 1) were optimized using the standard Hull cell method. By adding HCl and $NaHCO_3$ in the appropriate proportions, the pH of the bath was optimized from a pH meter. The anode was made of pure zinc metal, and the cathode was made of low-carbon steel panels. The whole electrodeposition process took place at room temperature. After the electrodeposition process, the plate was taken out of the electrolytic solution and immersed in one percent HNO_3 for 3 to 5 seconds before being washed with water.

The cyclic voltammetric (CV) investigations were carried out using CHI660D electrochemical equipment by only a three-electrode configuration. The working electrode was a 0.08 cm^2 steel electrode, the counter electrode was a platinum wire, and the reference electrodes were saturated calomel. Each investigation began with the working electrode being cleaned up to a glass shine using 0.05 μm alumina.

Table 1. Optimized bath composition and operating conditions

Bath Constituents	Concentration (gL^{-1})	Operating conditions
$ZnSO_4.7H_2O$	240	Anode: zinc plate (99.9%)
$NiSO_4.5H_2O$	10	Cathode: mild steel
Na_2SO_4	40	pH: 3.5, temperature: 298K
H_3BO_3	8	Plating time :10 minutes
CTAB	2	Cell current : 1A
DHB	0.083	Current density:1-5 A dm^{-2}

The coating's different characteristics and corrosion resistance were examined on these Zn-Ni-coated steel sheets. The corrosion behavior in a 3.5 percent sodium chloride was studied with electrochemical impedance spectroscopy (EIS) and Tafel extrapolation with three electrodes on the electrochemical workplace CHI608D (CH Instruments, Austin, USA). Zn-Ni coatings with a surface area of 1 cm^2 were made as the working electrodes, the reference electrode was calomel, and the counter electrode was platinum. The microstructural analysis of the coatings was performed using a

scanning electron microscope (SEM, model ZEISS). The microstructures of the Zn-Ni alloy were studied using X-ray diffraction (RIGAKU) technique with Cu Ka (k = 1.5406 A°) as the radiation source.

RESULTS AND DISCUSSION

Electrolytic Bath Optimization and Coating Composition: The Zn-Ni coatings developed from Hull cell studies were dull deposits with current densities ranging from 1 to 5 Adm^2. Organic additives such as 2, 5 dihydroxy benzaldehyde (DHB) were added to the electrolytic bath to enhance the nature of the electrodeposit.

Initially, with a low additive concentration, greyish dull deposits developed at lower current densities, whereas charred deposits formed at higher current densities. To optimize the electrolytic solution, the amount of the additional agents in the electrolytic solution gradually raised with each electrode position. DHB functions as a brightener, decreasing the rate of zinc ion reduction and zinc solubility while enhancing the hydrogen evolution process [**16**]. The deposit's nature was improved and considered as optimal. An organic additive such as 2, 5 dihydroxy benzaldehyde (DHB) was added to the electrolytic bath.

It was observed that the reason for adding boric acid was to regulate the variation in the number of hydrogen ions, resulting in pH changes in the electrolytic solution. To determine the ideal amount of boric acid, the quantity of boric acid was changed, while keeping the quantities of other additional agents constant. At 30 g L^{-1} boric acid, a bright coating was obtained. The inclusion of boric acid significantly enhanced the quality of the deposit [**11**].

Cyclic Voltammetric studies: The cyclic voltammetric method was applied to assess the effect of DHB on the co-deposition of Zn-Ni alloy (Figure 1). A cathodic and three oxidation peaks (p1, p2, and p3) can be seen on the cyclic voltammogram for an optimized bath without DHB, during the electrochemical oxidation of alloys [**17**], multiple peaks at various stages appear as the metals dissolve in the alloy. Voltammetric curves, therefore, give information on the different stages of Zn-Ni deposits.

In the absence of DHB, three anodic peaks associated with the dissolution of the η-phase, δ-phase (Ni_3Zn_{22}), and γ-phase (Ni_5Zn_{21}) of the Zn-Ni alloy deposit were produced. Zinc dissolution from δ- and γ-phases is represented by the first peak (p1) at -0.66V and the second peak (p2) at -0.46V. The dissolution of nickel from,η, γ and δ phases[**18**] is characterized by the third peak (p3) at higher noble potential.

Due to the additive's fractional absorption, two cathodic peaks (A’ and A2) were seen during the reduction of zinc ions in the presence of DHB.As additive molecules adsorb to an electrode's surface, a portion of the active surface is blocked ($\theta_{blocked}$) where the initial reducing process take place [**19**]. Hence, only a small portion of the active surface ($1-\theta_{blocked}$) was unblocked, allowing zinc ion reduction to proceed. Thus, in the absence of DHB, the current density for zinc ion reduction falls. DHB dissolves as the over potential rises, enabling zinc ions to be reduced at the active surface. On reversing the potential scan, one anodic peak of decreasing intensity is found, which is indicative of the solubility of zinc and nickel from δ- and γ-phases. Our research shows DHB partly adsorbs on the electrode, reducing rate of zinc ion reduction and promoting the generation of improved uniformity in brighter deposit

Potentiodynamic polarization and Electrochemical impedance studies: Previous investigations revealed that the plating of Zn-Ni alloys had better resistance to corrosion compared to all the other metals dissolved in zinc. The electroplating bath with DHB and other chemicals added results in a

bright, fine-grained deposit and boosts the corrosion resistance of the Zn-Ni alloy coating. Moreover, because of variations in the chemical composition of the coating, the protection capacity of the alloy coating varies with deposition, current, density, and thickness at the same current density. As a result, the influence of DHB, current density, and thickness on the protective ability of the optimized bath deposit must be investigated.

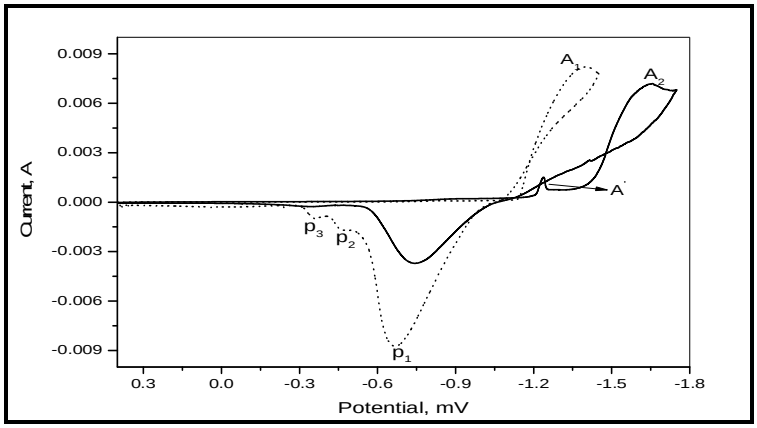

Figure 1. Typical cyclic voltammograms recorded with (solid line) and without (dot line) of DHB in the bath solution.

The Tafel curves for dull and bright Zn-Ni alloy coatings produced at 4 A dm^{-2} in the presence and absence of DHB, respectively, are shown in figure 2. The Tafel curves' corrosion parameters are included in table 2. When compared to dull deposits, the value of I_{corr} dropped, and a decreased corrosion rate had been seen for bright deposits. Hence, the bright Zn-Ni coating has greater corrosion resistance.

Table 2. Corrosion parameters derived from Tafel curve

Coating	E_{corr} (V/SCE)	I_{corr} (μAcm^{-2})	βc (V^{-1})	βa (V^{-1})	Corrosion rate ($\mu g/ h^{-1}$)
Zn-Ni	-1.017	1.312	6.23	14.13	1.35
Zn-Ni + DHB	-0.986	0.729	6.89	18.214	0.76

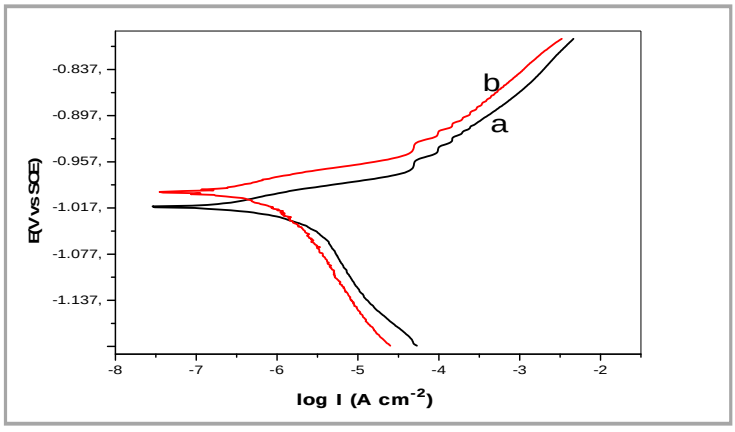

Figure 2. Typical Tafel plots of Zn- Ni alloy electrodeposits in 3.5 % NaCl solution obtained (A) in absence and (B) in presence of DHB in the bath solution.

The bright Zn-Ni alloy coating's high protection capacity is determined by its texture, shape, and chemical composition. The greater atom binding energy and the quick development of the protective

oxide layer in the fine-grained brilliant deposit make atom oxidation more difficult. The co-deposition of nickel with zinc in the coating promotes the deposit's corrosion resistance. Moreover, the microstructure of the bright Zn-Ni deposit includes δ -phase and γ-phase showing high corrosion resistance.

Impedance spectroscopy was used to investigate the electrochemical properties of electrodeposited Zn-Ni alloys. Figure 3 shows a study of Nyquist plots of Zn-Ni alloy deposits formed with and without DHB in the bath solution. The charge transfer resistance Rct value of deposits obtained with and without DHP was approximately 524.5 and 2966.5 Ωcm^2, respectively. The greater Rct value for the bright deposit relative to the dull deposit indicates that the bright coating decreases ion diffusion and can reduce low-carbon steel corrosion rate. This is consistent with the findings of potentiodynamic polarisation studies.

Further impedance modulus $|Z|$ vs frequency bode plot shows that Zn-Ni bright deposit has a higher $|Z|$ value (Figure 4a) and the frequency vs phase angle bode plot shows an increase in phase angle for Zn-Ni bright deposit (Figure 4b). These outcomes are consistent with the Tafel and Nyquist plot analyses.

Table 3. Corrosion parameters derived from impedance curve

Deposits	Rs ($\Omega cm^{2)}$	CPE (μFcm^{-2})	Wsr	R_p (Ωcm^2)
Zn-Ni	6.14	6.11	246.14	524.5
Zn-Ni + DHB	4.65	5.6	190.77	2966.5

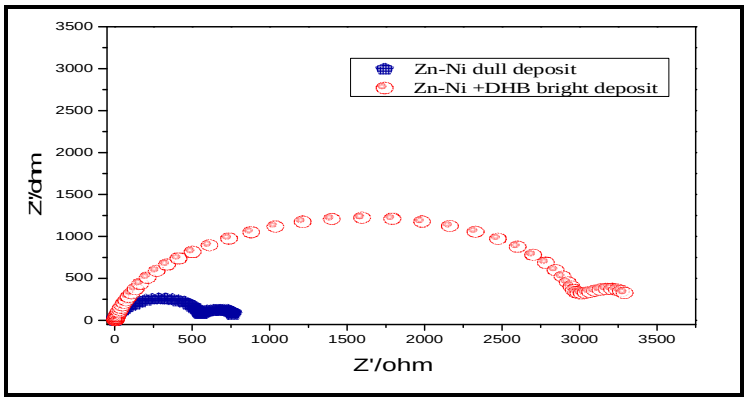

Figure 3. Nyquist plots of Zn-Ni alloy electrodeposits in a solution of 3.5% NaCl.

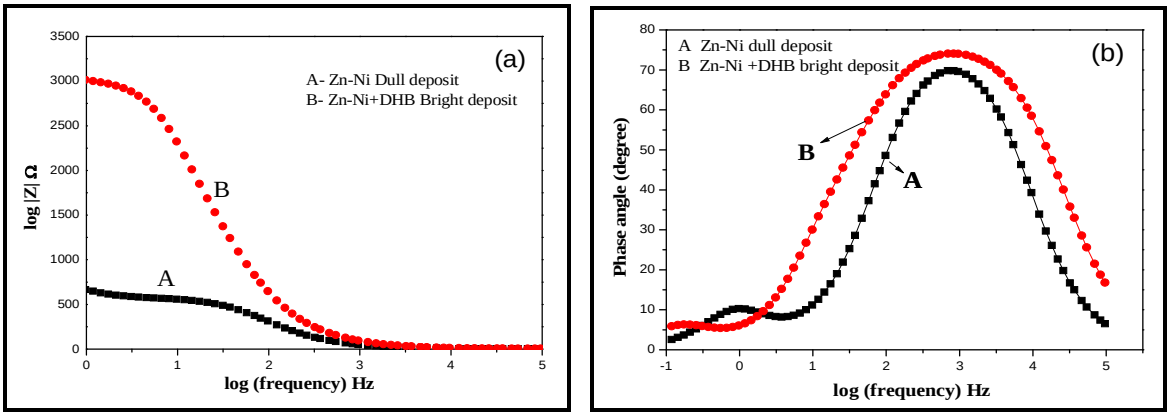

Figure 4. Bode plot of Zn-Ni alloy electrodeposits (a) log modulus Z vs log *f* (b) phase angle vs log *f*.

X-ray diffraction (XRD) analysis: Figure 5 shows the generation of line matching to η-phase Zn-Ni and extra lines which could be referenced using a γ-Ni_5Zn_{21} and δ-Ni_3Zn_{22}. When the concentration of DHB increases from 0.0 to 1.2 mM, the intensity of the γ-Ni_5Zn_{21} (330) phase line decreases while the intensity of the δ-Ni_3Zn_{22} (004) phase line increases. The presence of more δ-Ni_3Zn_{22} phase in the deposit improves the corrosion resistance of the alloy [**20**]. As a result of these findings, the Zn-Ni deposits produced in the presence of DHB demonstrated greater corrosion resistance.

The texture coefficient for each peak in the diffraction patterns was computed to determine the Zn-Ni alloy coatings' preferred orientation (Figure 6). The appropriate Tc values were illustrated as a bar chart in figure 5. The dull deposit contains 44.28% Zn-Ni alloy crystallites that are oriented parallel to the (330) plane. As a result, the (330) plane was the dull deposit's preferred orientation. In the case of Zn-Ni bright coatings, 49.9% of crystallites are parallel to the (004) plane and 38.96% are parallel to the (622) plane. As a result, (004) and (622) are the recommended as bright deposit preferred orientations. The preferential adsorption of DHB on different crystallographic planes alters the preferred orientation of (330) to (004) deposition and (622).

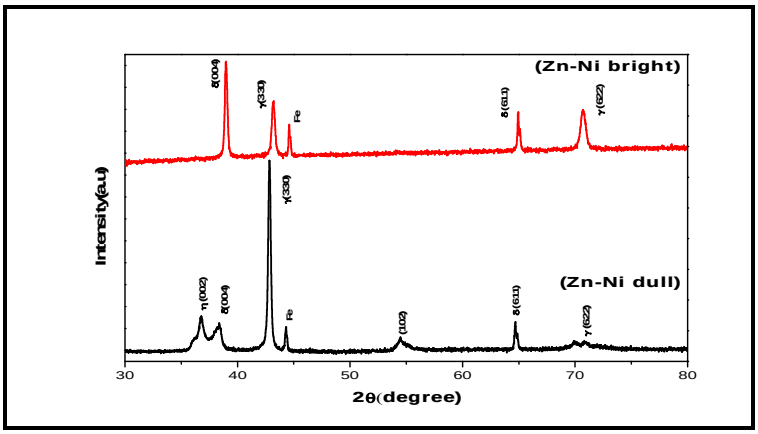

Figure 5. Zn-Ni alloy electrodeposit X-ray diffraction patterns.

Surface morphology and Reflectance: SEM images of the dull and bright deposits obtained in the absence and presence of DHB are shown in Figure 6. The dull deposition was coarse-grained, with brittle, unevenly scattered hexagonal plates. The bright deposit, on the other hand, had a small, homogeneous, uniform surface and was packed with no pores. This suggests that DHB encourages grain size refinement by increasing the number of nucleation sites and decreasing nuclei development during deposition.

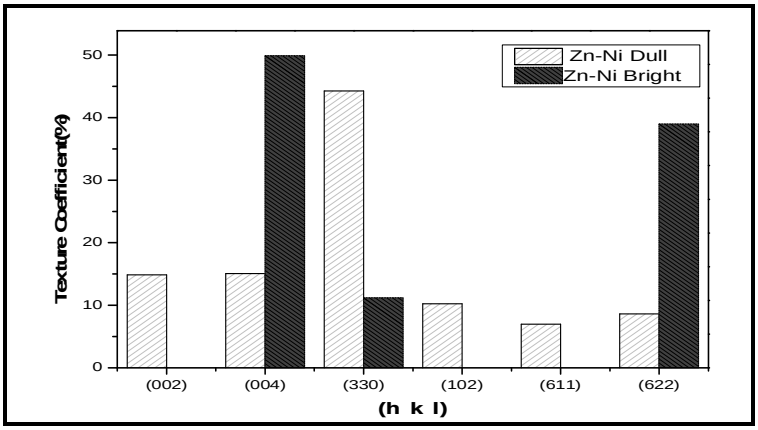

Figure 6. Tc values for dull and bright Zn-Ni alloy deposits as a function of crystallographic plane.

Figure 7 displays the optimal reflectivity and extent of total reflectivity for Zn-Ni alloy coatings with and without DHB for visible radiations. The addition of DHB to the bath solution enhanced the amount of mirror reflection in the visible zone, as shown in figure 7. At various points on the exterior, the Zn-Ni alloy coating displays only a 3 to 5% variation in overall reflectivity for visual light. Our findings demonstrated that DHB is an effective brightener for Zn-Ni alloy coatings.

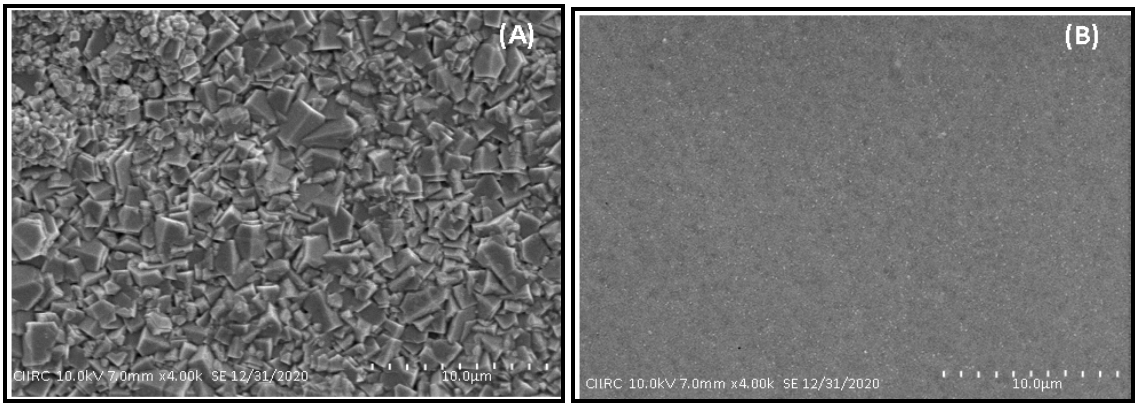

Figure 7. SEM images of Zn-Ni alloy electrodeposits made in the bath solution without (A) and with (B) DHB.

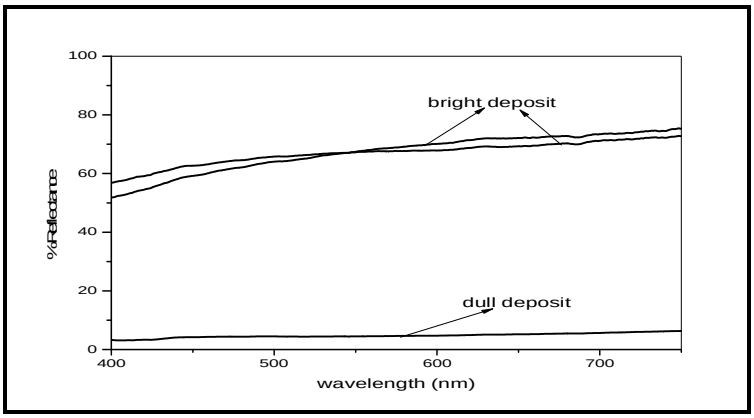

Figure 8. The reflectance spectra of Zn-Ni alloy electrodeposits formed inthe bath solution with Bright and dull deposit.

APPLICATION

A suitable acid sulphate bath is developed for electroplating of Zn-Ni alloy coatings on a mild steel using DHB as a brighter.

CONCLUSION

DHB is an organic additive used in the electroplating bath of Zn-Ni alloys for bright coatings. The anodic peaks of cyclic voltammetric curves reveal that and δ-phases are present in Zn-Ni alloy deposits and the decrease in peak intensity supports the reduction in Zn-Ni phase dissolution. The existence of γ-Ni_5Zn_{21}, δ-Ni_3Zn_{22} phases, is confirmed by XRD analysis, and (004) and (622) are the preferred orientations of the bright deposit. Corrosion experiments indicate that Zn-Ni coatings formed in the presence of DHB had high protection against corrosion and a minimum corrosion rate. SEM and reflectance measurements confirm that the presence of organic additives promotes the production of uniform and bright deposits.

REFERENCES

[1]. K. K. Maniam, S. Paul, Corrosion Performance of Electrodeposited Zinc and Zinc-Alloy Coatings in Marine Environment, *Corros. Mater. Degrad.*, **2021,** 2, 163–189.

[2]. I. H. Karahan, A study on electrodeposited Zn1-x Fe x alloys, *J. Mater. Sci.*, **2007,** 42, 10160–10163.

[3]. R. S. Bhat, S. M. Shetty, N. A. Kumar, Electroplating of Zn-Ni Alloy Coating on Mild Steel and Its Electrochemical Studies, *J. Mater. Eng. Perform.*, **2021,** 30, 8188–8195.

[4]. E. Beltowska-Lehman, P. Ozga, Z. Swiatek, C. Lupi, Electrodeposition of Zn-Ni protective coatings from sulfate-acetate baths, *Surf. Coatings Technol.*, **2002,**151–152, 444–448.

[5]. D. Verma Atul,*Certain distance degree based Topol. indices Zeolite LTA Fram.*, **2018**,11–14.

[6]. M. M. Abou-Krisha, A. G. Alshammari, F. H. Assaf, F. A. El-Sheref, Electrochemical behavior of Zn–Co–Fe alloy electrodeposited from a sulfate bath on various substrate materials, *Arab. J. Chem.*, **2019,**12, 3526–3533.

[7]. G. Roventi, R. Fratesi, R. A. Della Guardia, G. Barucca, Normal and anomalous codeposition of Zn-Ni alloys from chloride bath, *J. Appl. Electrochem.*, **2000**, 30, 173–179.

[8]. Z. Feng, Q. Li, J. Zhang, P. Yang, M. An, Electrochemical Behaviors and Properties of Zn-Ni Alloys Obtained from Alkaline Non-Cyanide Bath Using 5,5′-Dimethylhydantoin as Complexing Agent, *J. Electrochem. Soc.*, **2015,** 162, D412–D422.

[9]. Y. Addi, A. Khouider, Zinc-Nickel Codeposition in Sulfate Solution Combined Effect of Cadmium and Boric Acid, *Int. J. Electrochem.*, **2011**, 1–7.

[10]. Ravindran, V. V. S. Muralidharan, Zinc-Nickel Alloy Electrodeposition–Influence of Triethanolamine, *Port. Electrochim. Acta,* **2007,** 25, 391–399.

[11]. J. S. Kavirajwar, S. Basavanna, B. K. Devendra, An investigation on corrosion properties of bright Zn-Ni alloy coated mild steel, *Electrochem. Sci. Adv.*, **2021,** 1–8.

[12]. P. Díaz-Arista, Y. Meas, R.Ortega, G. Trejo, Electrochemical and AFM study of Zn electrodeposition in the presence of benzylideneacetone in a chloride-based acidic bath, *J. Appl. Electrochem.*, **2005,** 35, 217–227.

[13]. R. Bernasconi, Electrodeposition from Deep Eutectic Solvents, *Prog. Dev. Ion. Liq.*, **2017.**

[14]. C. An, K. An, C. Liu, X. Qu, Adsorption behavior of 3-phenylacrylaldehyde on a tin surface during electroplating, *Int. J. Electrochem. Sci.*, **2017**, 2, 10542–10552.

[15]. E. Rudnik, G. Chowaniec, Effect of Organic Additives on Electrodeposition of Tin From Acid Sulfate Solution, *Metall. Foundry Eng.*, **2018**, 44, 41.

[16]. G. Mao, M. Kilani, M. Ahmed, Review-Micro/Nanoelectrodes and Their Use in Electrocrystallization: Historical Perspective and Current Trends, *J. Electrochem. Soc.*, **2022**, 169, 022505.

[17]. S. Basavanna, Y. Arthoba Naik, Study of the effect of new brightener on Zn-Ni alloy electrodeposition from acid sulphate bath, *J. Appl. Electrochem.*, **2011**, 41, 535–541.

[18]. M. Abdallah, B. A. Al Jahdaly, M. M. Salem, A. Fawzy, E. M. Mabrouk, Electrochemical behavior of nickel alloys and stainless steel in HNO3 using cyclic voltammetry technique, *J. Mater. Environ. Sci.*, **2017**, 8, 1320–1327.

[19]. K. O. Nayana, T. V. Venkatesha, Effect of ethyl vanillin on ZnNi alloy electrodeposition and its properties, *Bull. Mater. Sci.*, **2014,** 37, 1137–1146.

[20]. S. Anwar, Electrochemical and Corrosion Behavior of Electrodeposited Zn, Zn-Ni Alloy and Zn-Ni-TiO_2 Composite Coatings, **2021.**